NIH Public Access
Author Manuscript
Nature. Author manuscript; available in PMC 2011 February 1.

Published in final edited form as:
Nature. 2010 August 26; 466(7310): 1110–1114. doi:10.1038/nature09264.

Rb regulates fate choice and lineage commitment *in vivo*

Eliezer Calo, **Jose A. Quintero-Estades**, **Paul S. Danielian**, **Simona Nedelcu**, **Seth D. Berman**, and **Jacqueline A. Lees**
David H. Koch Institute for Integrative Cancer Research @ MIT, Massachusetts Institute of Technology, 77 Massachusetts Ave, Cambridge, MA 02139, USA.

Abstract

Mutation of the *RB-1* tumour suppressor occurs in one third of all human tumours and is particularly associated with retinoblastoma and osteosarcoma1. Numerous functions have been ascribed to the product of the human *RB-1* gene, pRB. The best known is pRB's ability to promote cell cycle exit through inhibition of the E2F transcription factors and the transcriptional repression of genes encoding cell cycle regulators1. In addition, pRB has been shown *in vitro* to regulate several transcription factors that are master differentiation inducers2. Depending on the differentiation factor and cellular context, pRB can either suppress or promote their transcriptional activity. For example, pRB binds to Runx2 and potentiates its ability to promote osteogenic differentiation program *in vitro*3. In contrast, pRB acts together with E2F to suppress PPARγ, the master activator of adipogenesis4,5. Since osteoblasts and adipocytes can both arise from mesenchymal stem cells, these observations suggest that pRB might play a role in the choice between these two fates. However, to date, there is no evidence for this *in vivo*. Here we use mouse models to address this hypothesis in the context of mesenchymal tissue development and tumorigenesis. Our data show that *Rb* status plays a key role in establishing fate choice between bone and brown adipose tissue *in vivo*.

Mutations in *RB1* (70–90% of cases) and *TP53* (50–70% of cases) are strongly associated with human osteosarcoma6 7. To model osteosarcoma in the mouse, we crossed $Rb^{fl/fl}$ (8) and $p53^{fl/fl}$ (9) conditional mutant mice with a transgenic line, *Prx1-Cre*10, which expresses Cre recombinase in uncommitted mesenchymal cells that contribute to bone, muscle, and both white and brown adipose tissue (Supplementary Figure 1a–c). The homozygous deletion of *Rb* and/or *p53* by *Prx1-Cre* yielded viable neonates with no detectable developmental defects (data not shown), allowing us to determine the affect of *Rb* and/or *p53* loss on sarcomagenesis (Figure 1a). The *Prx1-Cre;*$p53^{fl/fl}$ animals developed osteosarcoma (62%), rhabdomyosarcomas (15%) and/or undifferentiated sarcomas (12%). In contrast, deletion of *Rb* alone did not yield sarcomas. However, *Rb* mutation had a profound effect on the tumour spectrum of *Prx1-Cre;*$p53^{fl/fl}$ mice (Figure 1a,b): deletion of one *Rb* allele increased the frequency of osteosarcomas (to 92%), while mutation of both *Rb* alleles shifted the tumour spectrum away from osteosarcoma (now 18%) and towards hibernomas (91%; Supplementary figure 2). This propensity for brown fat, as opposed to

Users may view, print, copy, download and text and data- mine the content in such documents, for the purposes of academic research, subject always to the full Conditions of use: http://www.nature.com/authors/editorial_policies/license.html#terms

Correspondence and requests for materials should be addressed to J.A.L. (jalees@mit.edu).

Supplementary Information accompanies the paper on www.nature.com/nature.

Author contributions. E.C. conducted all the experiments in this study with assistance from J.A.Q-E. in the Rb re-introduction study, P.S.D. and S.D.B in the generation and analysis of compound mutant mouse strains and S.N. for the LSL-LacZ;Prx1-Cre embryo analysis. E.C. and J.A.L. were responsible for conceiving this study, interpretation of the data and manuscript preparation.

The authors have no competing interests.

NIH-PA Author Manuscript
NIH-PA Author Manuscript
NIH-PA Author Manuscript

NIH-PA Author Manuscript

NIH-PA Author Manuscript

NIH-PA Author Manuscript

white fat, tumors fits with prior studies showing that *Rb* loss promotes brown fat over white fat differentiation11,12,13. Genotyping confirmed that the tumour cells had undergone Cre-mediated recombination of *Rb* and/or *p53* (Figure 1c, data not shown). Moreover, it showed that the *Prx1-Cre*;$Rb^{+/fl}$;$p53^{fl/fl}$ tumours consistently retained the wildtype *Rb* allele (Figure 1c, data not shown). Thus *Rb* acts in a dose dependent manner to modulate the spectrum of tumours arising from p53-deficient, uncommitted mesenchymal stem cells: osteosarcomas predominant in the presence of *Rb*, while *Rb* loss strongly favours hibernoma formation.

Given that *Rb* loss in *p53* mutant uncommitted mesenchymal cells disfavours osteosarcoma formation, we also investigated the affect of *Rb* loss in a bone-committed progenitor. For this, we deleted *Rb* and/or *p53* using the *Osx-Cre* transgenic14 which uses *Osterix* promoter sequences to express Cre in the pre-oestoblast (Supplementary Figure 1d). In this model15, *Osx-Cre*;$p53^{fl/fl}$ mice specifically develop osteosarcoma (100%) while *Osx-Cre*;$Rb^{fl/fl}$;$p53^{fl/fl}$ develop osteosarcoma (53%), hibernomas (46%) and sarcomas (2%). We established cell lines from multiple (≥3) independent *Osx-Cre*;$p53^{fl/fl}$ and *Osx-Cre*;$Rb^{fl/fl}$;$p53^{fl/fl}$ osteosarcomas and discovered that the two genotypes have distinct differentiation properties (Figure 2, data not shown). The *Rb;p53* (*DKO*) osteosarcoma (OS) cell lines expressed mRNAs that are characteristic of bone and fat differentiation (Figure 2a). Indeed, their expression pattern more closely resembled that of mesenchymal stem cells (MSCs) than primary osteoblasts (Supplementary Figure 3). Accordingly, culture in the appropriate differentiation media induced these *DKO* cells to adopt either the adipogenic or osteoblastic fate (Figure 2a). In contrast, the *p53KO* OS cell lines closely resembled pre-osteoblasts based on their gene expression patterns, but these cells were unable to differentiate into either bone or fat (Figure 2a and Supplementary Figure 3). Since this differentiation block occurs in the p53-null OS cell lines, but not p53-deficient primary osteoblasts16 (Figure 4a), it likely reflects their transformed state. We used these *p53KO* OS cells to determine whether *Rb* loss was sufficient to alter the differentiation potential of blocked pre-oestoblasts by introducing control (*shLuc*) or *Rb*-specific (*shRb*) shRNAs. pRb was readily detectable in *shLuc-p53KO*, but not *shRb-p53KO*, OS cells (Figure 2b). Strikingly, without addition of differentiation media, pRb knockdown downregulated the bone-specific mRNA *Bsp* and upregulated the fat regulator *Pparγ* (Figure 2b). Accordingly, these *shRb-p53KO* OS cells were now able to differentiate into either bone or fat *in vitro* (Figure 2c). Moreover, when transplanted into nude mice, the *shRb-p53KO* OS cells formed more aggressive tumors than the parental *p53KO* OS cells, and these were of mixed lineage (fat, bone and undifferentiated sarcomas), in stark contrast to the undifferentiated osteoblastic tumours arising from either control *shLuc-p53KO* or parental *p53KO* OS cell lines (Figure 2d, Supplementary Figure 4, and data not shown). Thus, pRB loss is sufficient to over-ride the differentiation block of these p53-deficient, tumor cell lines and also expand their fate commitment to include the adipogenic state.

We also examined the consequences of reintroducing *Rb* into the *DKO* OS cells. For this, we induced pRb in confluence-arrested DKO cells using a doxocycline-inducible expression system (*DKO-*$Rb^{Dox\text{-}ON}$; Supplementary Figure 5). Remarkably, pRB restoration caused the *DKO* OS cells to adopt the differentiation state of the *p53KO* OS cell lines within two days: it induced down-regulation of adipogenic markers and up-regulation of osteogenic markers, and the cells were unable to differentiate into fat (Supplementary Figure 5). Thus removal or re-introduction of *Rb* appears sufficient to switch lineage specification between osteoblastic commitment and multipotency.

In vitro studies have shown that pRB can act with E2F to enforce transcriptional repression of *Pparγ*4,5, and also bind, and potentiate the transcriptional activity of, the osteogenic regulator RUNX23. We hypothesized that pRB's role in these processes might underlie *Rb*'s affect on adipogenesis versus osteogenesis. Thus, we used our *DKO-*$Rb^{Dox\text{-}ON}$ cells to

NIH-PA Author Manuscript

NIH-PA Author Manuscript

NIH-PA Author Manuscript

determine whether the presence or absence of pRb modulated these transcriptional regulators (Figure 3). First, we used chromatin-immunoprecipitation assays to investigate promoter regulation of *Pparγ* and representative Runx2-responsive genes *Coll1α* (Figure 3a) and osteocalcin (*Oc*; data not shown). pRb-induction caused both pRb and E2f4, the predominant repressive E2F, to be recruited to the *Pparγ* promoter (Figure 3a) and this correlated with *Pparγ* mRNA downregulation (Figure 3a). Contemporaneously, pRb bound to *Coll1α* and *Oc* and this was accompanied by increased promoter occupancy of Runx2 and upregulation of *Coll1α* and *Oc* mRNAs (Figure 3a, data not shown). Importantly, these changes in *Pparγ*, *Coll1α* and *Oc* regulation were all detected within 2 days of pRb induction and without addition of differentiation-inducing media. In addition, we found that Runx2 associated with pRb in the *p53KO*, but not the *DKO*, OS cells and its transcriptional activity was 8 fold higher in the former, versus the latter, population (Figure 3b). Thus the presence or absence of pRb directly modulates the levels and activity of Pparγ and Runx2 in accordance with the preferential commitment of our OS cell lines to the osteogenic versus the adipogenic lineage.

The preceding experiments establish a clear role for pRb in fate commitment bias *in vivo* and *in vitro*. However, since this analysis was conducted in p53-deficient cells, it is unclear whether *Rb* alone is sufficient to determine this plasticity or whether transformation is also required. To address this, we isolated primary osteoblasts from the calvaria of $Rb^{fl/fl}$, $p53^{fl/fl}$ or $Rb^{fl/fl}$;$p53^{fl/fl}$ e18.5 embryos. We brought these cells to confluence, to minimize the influence of altered proliferation, infected them with adenoviruses expressing Cre or a GFP control and then assayed differentiation. As expected, the control infected osteoblasts were able to undergo osteogenesis but not adipogenesis (Figure 4a; data not shown). Similarly, p53 loss had no effect on this fate commitment16 (Figure 4a). In stark contrast, deletion of *Rb*, either alone or together with *p53*, allowed these cells to adopt either the bone or fat lineage (Figure 4a; data not shown). This switch to multipotency correlated with the significant upregulation of adipogenic markers prior to the induction of differentiation (Figure 4b). Thus, pRB-loss is sufficient to alter the fate commitment in otherwise wildtype calvarial osteoblasts.

In vitro culture can modulate the plasticity of cells. Thus, we wished to examine *Rb*'s role in fate choice *in vivo*. For this, we employed a third transgenic strain, *Meox2-Cre*, which expresses Cre in the embryo proper from e6.517. *Meox2-Cre;*$Rb^{fl/fl}$ embryos survive to birth18. We isolated wildtype (*Meox2-Cre;*$Rb^{+/+}$) and *Rb* mutant (*Meox2-Cre;*$Rb^{fl/fl}$) littermates at e15.5 and e18.5 and examined both bone and brown fat development. First, there was a significant reduction in the level of calcified bone matrix in both the calvaria and long bones of *Rb* mutant versus wildtype embryos19 (Figure 4c). Moreover, qPCR analysis established that *Runx2* mRNA was present at appropriate levels in the *Rb* mutant e18.5 calvarial osteoblasts, but there was a downregulation of other bone markers and a clear upregulation of fat-associated mRNAs (Figure 4c). In parallel, we found that the level of brown fat was dramatically increased in the e18.5 *Rb* mutant versus the wildtype controls (Figure 4d and Supplementary Figure 6). Thus, *Rb* loss in an, otherwise wildtype, embryo impairs bone differentiation and expands the fat compartment.

Our data establish a clear role for pRB in determining the fate choice of mesenchymal progenitors and the lineage commitment of pre-osteoblasts. This occurs both *in vitro* and *in vivo* and irrespective of whether these cells are transformed or otherwise wildtype. *In vivo*, *Rb*-loss favours adipogenesis over osteogenesis to the extent that it can reduce the levels of calcified bone and greatly increase the levels of brown fat. Moreover, *Rb*-loss in pre-osteoblasts is sufficient to disfavour commitment to the osteogenic state and restore multipotency. It is possible that *Rb* loss allows expansion of a rare multipotent progenitor population that exist within the pre-osteoblast compartment. Alternatively, *Rb* loss could be

NIH-PA Author Manuscript

NIH-PA Author Manuscript

NIH-PA Author Manuscript

actively reprogramming the pre-osteoblasts by driving either trans-differentiation to the adipogenic lineage or true de-differentiation to the multipotent progenitor stage. Between the two reprogramming models we favour de-differentiation based on both the expression of multi-lineage differentiation markers in the DKO OS cells (Supplementary Figure 3) and the broadening of the tumor spectrum from solely oesteosarcomas in the *Osx-Cre;p53*$^{fl/fl}$ animals to include not only osteosarcomas and hibernomas but also sarcomas in the *Osx-Cre;Rb*$^{fl/fl}$*;p53*$^{fl/fl}$ mice. Finally, our data offers potential insight into the cell of origin for osteosarcomas. Specifically, given the high frequency of *RB-1* mutations in human osteosarcoma, we were surprised to find that *Rb* mutation predisposes mesenchymal cells away from the osteoblastic state. Given this finding, we speculate that *RB-1* mutant osteosarcomas are likely to arise from more committed osteoblastic lineages than from uncommitted mesenchymal progenitors. In this setting, *RB-1* loss could enable de-differentiation and thereby synergize with other mutations to promote tumorigenesis.

Methods Summary

Animal maintenance and histological analyses

Animal procedures followed protocols approved by MIT's Committee on Animal Care. The *Rb*$^{fl/fl}$ (8), *p53*$^{fl/fl}$ (9), *Osx1-GFP::Cre*14, *Prx1-Cre*10, *Meox2-Cre*17 and *Rosa26-LSL-lacZ* (Jackson Labs) animals were maintained on a mixed genetic background. The transplant assays were conducted in NOD/SCID mice using 10^4 cells. Protocols for tissue sectioning and skeletal staining are described in the additional methods section.

OS cell lines and primary osteoblast generation and analysis

Osteoblast cell lines and primary osteoblasts were generated and analyzed as described in the additional methods section or previously19. Knock-down of *Rb* in the *p53KO-OS* cells was achieved using the pMLP-miR30-based shorthairpin (*Rb* targeted sequence: CACGGACGTGTGAACTTATATA). Adenoviruses expressing Cre or GFP were provided by the U. of Iowa Gene Transfer Vector Core. For immunoprecipitations and immunoblotting, proteins were extracted with a Triton X-100 based buffer and quantified by the BCA assay reagent (Pierce, Inc). Antibodies were from Santa Cruz Biotechnology [pRb (H-153), E2F1 (C-20), and E2F4 (C-20)], BD Pharmingen (pRb), Ambion (GAPDH) and MBL (Runx2). Dual luciferase assays were performed as described by the manufacturer (Promega). The Runx2 reporter p6OSE2-Luc and control p4Luc were provided by Dr. Gerard Karsenty.

Additional Methods

Mouse genotyping

The *Rb* conditional band was detected using the primers 5'lox: 5'-CTCTAGATCCTCTCATTCTTC-3' and 3'lox: 5'-CCTTGACCATAGCCCAGCAC-3'. Primer Rbcre3.2 (5'-GGTTAATGAAGGACTGGG-3') was used in conjunction with primer 5'lox to detect the recombined band. To identify the p53 conditional allele we used primer p53A: 5'-CACAAAAACAGGTTAAACCCAG-3' and primer p53B: 5'-AGCACATAGGAGGCAGAGAC-3'. The recombined allele was detected using primer p53A in conjunction with primer p53D: 5'-GAAGACAGAAAAGGGGAGGG-3'.

Tumor monitoring and analysis

The criteria for euthanasia (by CO2 inhalation) were a total tumor burden of $2cm^3$, tumor ulceration/bleeding, signs of infection, respiratory distress, impaired mobility, ≥20% reduction in body weight or general cachexia. All tissues were collected and hip bones, femurs and tibias were separated and fixed overnight in PBS with 3.7% formaldehyde. Soft

NIH-PA Author Manuscript

NIH-PA Author Manuscript

NIH-PA Author Manuscript

tissues were transferred into 70% ethanol and dehydrated via an ethanol series prior to embedding in paraffin for sectioning. Tissues containing bone was either decalcified in 0.46M EDTA, 2.5% Ammonium Hydroxide pH 7.2 for two weeks then processed for paraffin sectioning. All paraffin embedded sections were cut at 5μm, dewaxed and stained with H&E. Sirius red staining was performed by treating sections briefly stained with hematoxylin with 0.1% Sirius red in saturated picric acid (Electron Microscopy Sciences) for one hour, washing in 5% v/v glacial acetic acid and then dehydration in ethanol/xylene prior to mounting.

Immunohistochemistry (IHC)

Runx2 IHC was performed using a modified citric acid unmasking protocol. Briefly, slides were deparaffinized in xylene and rehydrated through ethanol. Slides were boiled for 30 min in citrate buffer, pH 6.0, and then cooled in running tap water. Slides were then washed in PBS for 5 min followed by inactivation of endogenous peroxidases by incubation 0.5% H_20_2 in methanol. Slides were blocked in 10% Goat Serum for 1 h at room temperature. Primary antibody (MBL anti-Runx2 Clone 8G5) was diluted 1:200 in PBS 0.15% Triton and incubated overnight at 4 °C. The following day, slides were washed three times in PBS. Secondary antibodies (Vectastatin ABC kits, Vector laboratories) were diluted 1:500 in PBS containing 0.4% Goat Serum and detected using a DAB substrate (Vector Laboratories). All samples were counterstained with hematoxylin.

Skeletal Staining

Embryos were sacrificed, skinned and eviscerated. The remaining tissue was fixed in 95% ethanol for 4 days, transferred to acetone for 3 days, and subsequently transferred to staining solution of 0.015% Alcian blue 8GX (Sigma), 0.005% alizarin red S (Sigma), and 5% glacial acetic acid in ethanol at 37°C for 2 days and at room temperature for a one more day. Tissue was cleared in 1% potassium hydroxide for several days and then stored in glycerol.

Generation of osteosarcoma cell lines

Osteosarcomas were dissected, minced, filtered through a 70μm filter, and plated in normal growth medium (10% FBS in DME, 1% P/S, L-glutamine) to generate the OS cell lines. Cells were passaged as they reached confluence. For RNA purification, cells were rinsed 2× with PBS, and RNA extraction was performed using RNAeasy kit (Quiagen). First-strand cDNA was transcribed from 1 μg of RNA using Superscript III reverse transcriptase (Invitrogen) following the manufacturer's instructions. Quantitative RT-PCR with 20 to 100 ng cDNA was done using SYBR Green (Applied Biosystems). Reactions were run on the ABI Prism 7000 Sequence Detection System and analyzed using the 7000 SDS software. Primers used for qPCR were: Alkaline Phosphatase (F) TCTCCAGACCCTGCAACCTC and (R) CATCCTGAGCAGACCTGGTC; Col1a1 (F) CGAGTCACACCGGAACTTGG and (R) GCAGGCAGGGCCAATGTCTA; Osteocalcin (F) CTCTGTCTCTCTGACCTCACAG and (R) CAGGTCCTAAATAGTGATACCG; Osteopontin (F) TGCTTTTGCCTGTTTGGCAT and (R) TTCTGTGGCGCAAGGAGATT; Runx2 (F) TGAGATTTGTGGGCCGGA and (R) TCTGTGCCTTCTTGGTTCCC; Ap2 (F) ATCCCTTTGTGGGAACCTGGAA and (R) ACGCTGATGATCATGTTGGGCT; C/ebp α (F) CAAGAACAGCAACGAGTACCG and (R) GTCACTGGTCAACTCCAGCAC; Pparγ (F) GAGCTGACCCAATGGTTGCTG and (R) GCTTCAATCGGATGGTTCTTC; Srebp-1c (F) GGAGCCATGGATTGCACATT and (R) GCTTCCAGAGAGGAGGCCAG; Ucp-1 (F) AGCCGGCTTAATGACTGGAG and (R) TCTGTAGGCTGCCCAATGAAC; Pgc-1 (F) GTCCTCACAGAGACACTGGA and (R) TGGTTCTGAGTGCTAAGACC; Nbrf-1 (F) CGGCACCTAGCGCCCGG and (R) CGGCACCTAGCGCCCGG; MyoD (F) CGCCACTCCGGGACATAG and (R) GAAGTCGTCTGCTGTCTCAAAGG; Prdm16 (F) GACCACGGTGAAGCCATTC and (R) GCGTGCATCCGCTTGTG; Taz (F)

NIH-PA Author Manuscript

NIH-PA Author Manuscript

NIH-PA Author Manuscript

GTCACCAACAGTAGCTCAGATC and (R) AGTGATTACAGCCAGGTTAGAAAG; and Gapdh (F) CAAGGTGGCAGAGGCCTTT and (R) TCCAGCTGCTCAATGGACGCATTT.

Calvarial Osteoblasts Preparation and Culture

Calvaria from embryonic day 18.5 embryos were removed and carefully cleaned in sterile PBS from contaminating tissue. Then treated with several rounds of collagenase/trypsin digestion at 37°C, and plated onto six-well plates for 2 days in αMEM with 10% fetal bovine serum and penicillin/streptomycin. For differentiation, 3.5×10^5 cells were plated onto a well of a 6-well tissue culture plates. Upon reaching confluence, calvarial osteoblasts were treated with medium supplemented with 50 μg/mL of ascorbic acid and 10 mmol/L of β-glycerol-phosphate. Adenovirus (University of Iowa Gene Transfer Vector Core) was added to the medium at 100 plaque-forming units per cell and washed away 24 h later. To assay for calcium deposits, plates were stained with 1% alizarin red S solution (pH 5.0).

Chromatin Immunoprecipitation assay

Protein complexes were cross-linked to DNA by adding formaldehyde (Sigma, Inc.) to live cells to a final concentration of 1%. After incubation for 10 min at 37°C, glycine was added to give a final concentration of 0.125 M for 5 min. The cells were washed twice with PBS containing 1mM PMSF, scraped and pelleted. Nuclei were extracted with a 20mM Tris pH 8, 3 mM MgCl2, 20 mM KCl buffer containing protease inhibitors, pelleted by microcentrifugation and lysed with SDS lysis buffer (1% SDS, 10 mM EDTA, 50 mM Trischloride pH 8.1), containing protease inhibitors. The resulting chromatin solution was sonicated to generate 500–1000 bp DNA fragments. After microcentrifugation, the supernatant was diluted 1:10 with dilution buffer (0.01% SDS, 1.1% Triton X-100, 1.2 mM EDTA, 16.7 mM Trischloride pH 8.1, 167 mM NaCl, containing protease inhibitors), precleared with blocked protein A-positive Staph cells (Santa Cruz, Inc), and split into aliquots. These were incubated at 4°C for 12 to 16 hours with 5 μg antibody with rotation. Antibody-protein-DNA complexes were isolated by immunoprecipitation with blocked protein A-positive Staph A cells. Following extensive washing, bound DNA fragments were eluted and analyzed by Quantitative RT-PCR using the following primers: Pparγ proximal E2F site (F) ACGCGGAAGAAGAGACCT and (R) TCCTGTCAGAGTGTGACTTCTCCT; Pparγ distal E2F site (F) TCGCACTCAGAGCGGCAG and (R) AGGTCTCTTCCGCGTCCCT; Coll1a1 Runx2 site (F) TGCTTCCACGTTTACAGCTCTAAAG and (R) GTCAGGAAAGGGTCATCTGTAGTCC; Osteocalcin Runx2 site (F) GAGAGCACACAGTAGGAGTGGTGGAG and (R) TCCAGCATCCAGTAGCATTTATATCG.

Supplementary Material

Refer to Web version on PubMed Central for supplementary material.

Acknowledgments

We thank Tyler Jacks, Clifford Tabin and Andrew McMahon for providing key mutant mouse strains, Keara Lane for pCW22, Michael Hemann for the *Rb* shRNA, the U. of Iowa Gene Transfer Vector Core for the Adenoviral Cre and GFP vectors and Gerard Karsenty for p6OSE2-Luc and control p4Luc. We also thank Lees lab members, Siddhartha Mukherjee and Michael Hemann for input during this study. This work was supported by an NCI/NIH grant to J.A.L. who is a Ludwig Scholar at MIT.

NIH-PA Author Manuscript

NIH-PA Author Manuscript

NIH-PA Author Manuscript

References

1. Burkhart DL, Sage J. Cellular mechanisms of tumour suppression by the retinoblastoma gene. Nat Rev Cancer. 2008; 8(9):671. [PubMed: 18650841]
2. Korenjak M, Brehm A. E2F-Rb complexes regulating transcription of genes important for differentiation and development. Curr Opin Genet Dev. 2005; 15(5):520. [PubMed: 16081278]
3. Thomas DM, et al. The retinoblastoma protein acts as a transcriptional coactivator required for osteogenic differentiation. Mol Cell. 2001; 8(2):303. [PubMed: 11545733]
4. Fajas L, et al. The retinoblastoma-histone deacetylase 3 complex inhibits PPARgamma and adipocyte differentiation. Dev Cell. 2002; 3(6):903. [PubMed: 12479814]
5. Fajas L, et al. E2Fs regulate adipocyte differentiation. Dev Cell. 2002; 3(1):39. [PubMed: 12110166]
6. Clark JC, Dass CR, Choong PF. A review of clinical and molecular prognostic factors in osteosarcoma. J Cancer Res Clin Oncol. 2008; 134(3):281. [PubMed: 17965883]
7. Kansara M, Thomas DM. Molecular pathogenesis of osteosarcoma. DNA Cell Biol. 2007; 26(1):1. [PubMed: 17263592]
8. Sage J, et al. Acute mutation of retinoblastoma gene function is sufficient for cell cycle re-entry. Nature. 2003; 424(6945):223. [PubMed: 12853964]
9. Jonkers J, et al. Synergistic tumor suppressor activity of BRCA2 and p53 in a conditional mouse model for breast cancer. Nat Genet. 2001; 29(4):418. [PubMed: 11694875]
10. Logan M, et al. Expression of Cre Recombinase in the developing mouse limb bud driven by a Prxl enhancer. Genesis. 2002; 33(2):77. [PubMed: 12112875]
11. Hansen JB, et al. Retinoblastoma protein functions as a molecular switch determining white versus brown adipocyte differentiation. Proc Natl Acad Sci U S A. 2004; 101(12):4112. [PubMed: 15024128]
12. Scime A, et al. Rb and p107 regulate preadipocyte differentiation into white versus brown fat through repression of PGC-1alpha. Cell Metab. 2005; 2(5):283. [PubMed: 16271529]
13. Dali-Youcef N, et al. Adipose tissue-specific inactivation of the retinoblastoma protein protects against diabesity because of increased energy expenditure. Proc Natl Acad Sci U S A. 2007; 104(25):10703. [PubMed: 17556545]
14. Rodda SJ, McMahon AP. Distinct roles for Hedgehog and canonical Wnt signaling in specification, differentiation and maintenance of osteoblast progenitors. Development. 2006; 133(16):3231. [PubMed: 16854976]
15. Berman SD, et al. Metastatic osteosarcoma induced by inactivation of Rb and p53 in the osteoblast lineage. Proc Natl Acad Sci U S A. 2008; 105(33):11851. [PubMed: 18697945]
16. Lengner CJ, et al. Osteoblast differentiation and skeletal development are regulated by Mdm2-p53 signaling. J Cell Biol. 2006; 172(6):909. [PubMed: 16533949]
17. Tallquist MD, Soriano P. Epiblast-restricted Cre expression in MORE mice: a tool to distinguish embryonic vs. extra-embryonic gene function. Genesis. 2000; 26(2):113. [PubMed: 10686601]
18. Wu L, et al. Extra-embryonic function of Rb is essential for embryonic development and viability. Nature. 2003; 421(6926):942. [PubMed: 12607001]
19. Berman SD, et al. The retinoblastoma protein tumor suppressor is important for appropriate osteoblast differentiation and bone development. Mol Cancer Res. 2008; 6(9):1440. [PubMed: 18819932]
20. Barski A, Pregizer S, Frenkel B. Identification of transcription factor target genes by ChIP display. Methods Mol Biol. 2008; 455:177. [PubMed: 18463820]

NIH-PA Author Manuscript
NIH-PA Author Manuscript
NIH-PA Author Manuscript

a.

Genotype			Tumor Distribution (%)				Mice	Average Latency
Prx1	*Rb*	*p53*	RMS	SAR	OS	HIB	#	(days±SD)
+	fl/fl	+/+	0	0	0	0	7	428±130
+	+/+	fl/fl	15	12	**62**	0	19	342±101
+	+/fl	fl/fl	9	18	**92**	4	33	273±77
+	fl/fl	fl/fl	12	3	18	**91**	40	163±34

RMS=Rhabdomyosarcoma; SAR=Undifferentiated Sarcoma; OS=Osteosarcoma HIB=Hibernoma.

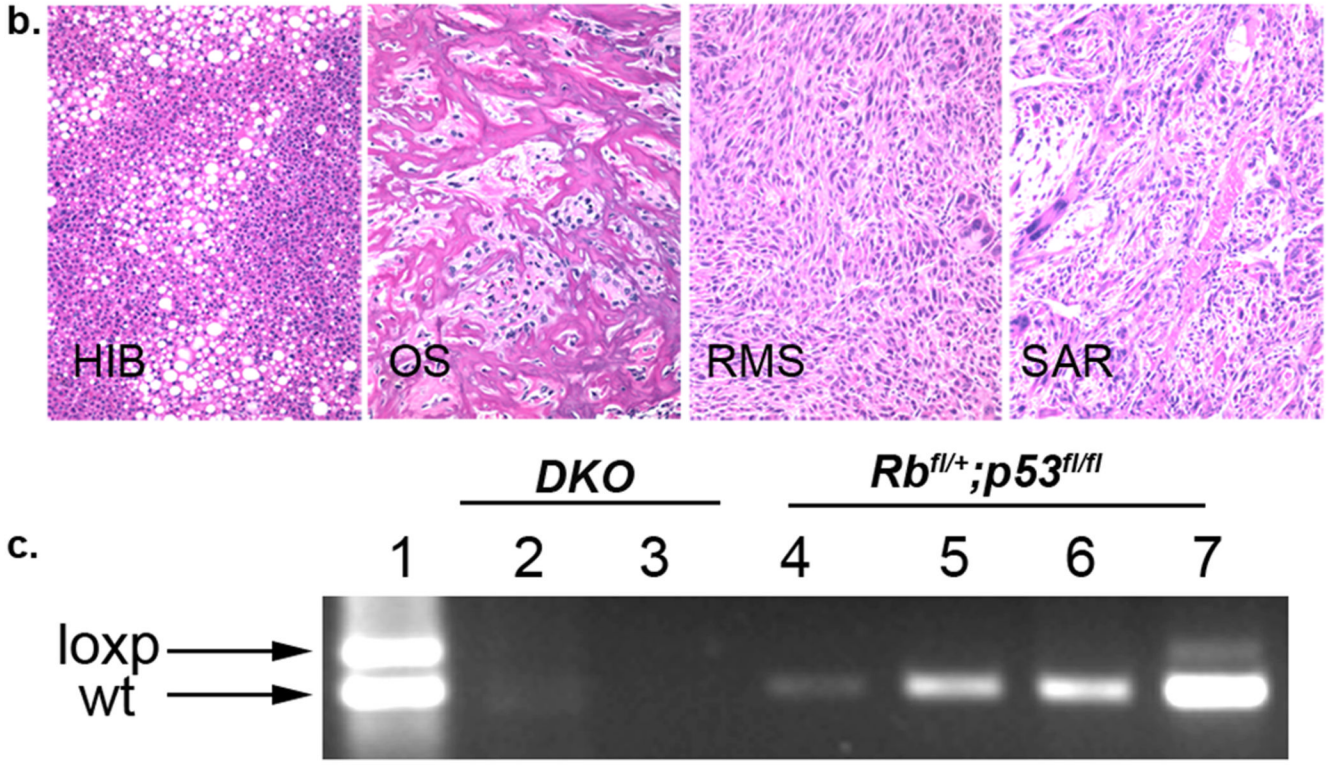

Figure 1. *Rb* cooperates with *p53* and modulates mesenchymal tumor fate in a dosage-dependent manner

a, Mesenchymal tumor distribution (percentage of animals analyzed up to 24 months of age) for *Prx1-Cre;Rb* and/or *p53* compound mutant animals. **b**, H+E staining of representative sarcomas (20× magnification). **c**, PCR genotyping to detect *Rb* wildtype (wt) and recombined conditional mutant (loxp) alleles in control $Rb^{fl/+};p53^{fl/+}$ tissues (lane 1) or cell lines derived from *Prx1-Cre;*$Rb^{fl/fl};p53^{fl/fl}$ (DKO) or *Prx1-Cre;*$Rb^{fl/+};p53^{fl/fl}$ osteosarcomas. Cell lines were cultured for ≥20 passages prior to genotyping to eliminate stromal cell contribution.

NIH-PA Author Manuscript

NIH-PA Author Manuscript

NIH-PA Author Manuscript

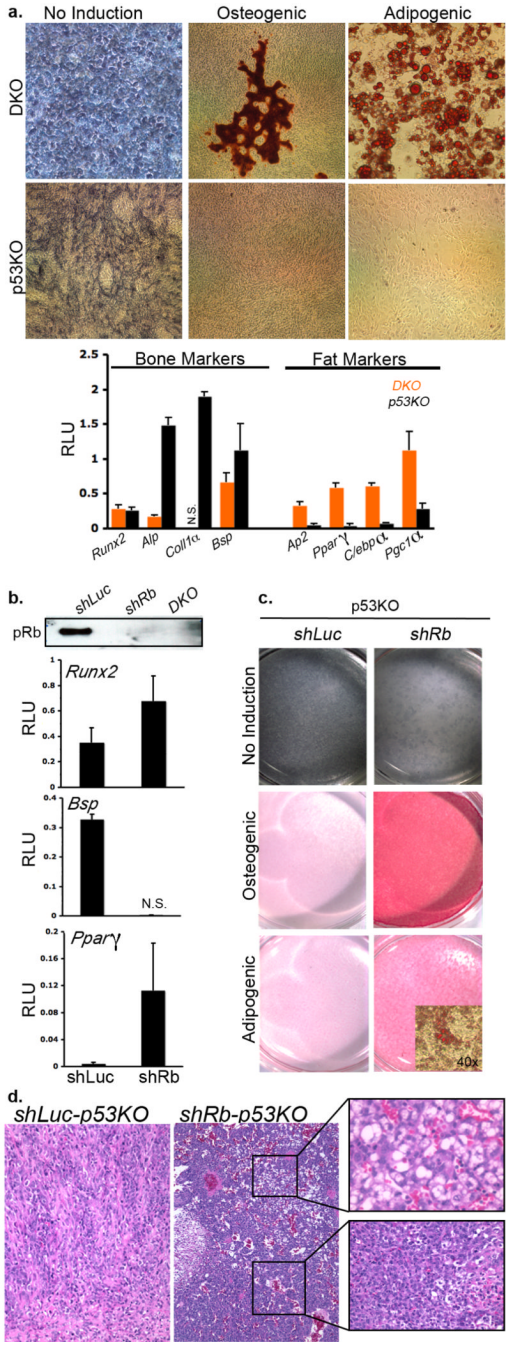

Figure 2. *Rb* regulates osteosarcoma-cell lineage plasticity *in vitro* and *in vivo*

The differentiation potential of 3 different *Osx-Cre;Rb*$^{fl/fl}$*:p53*$^{fl/fl}$ (*DKO*) and *Osx-Cre:p53*$^{fl/fl}$ (*p53KO*) OS cell lines was assessed 0, 7, 14, or 21 days after addition of differentiation media. **a**, Representative staining for: (left lane) alkaline phosphatase prior to differentiation induction; (middle lane) Alizarin Red to detect bone mineralization 14 days after culture in osteogenic-induction media and (right lane) Oil-Red-O to detect lipid droplets 14 days after culture in adipogenic-induction media. Expression of bone (*Runx2, Alp*, *Coll1a* and *Bsp*) and fat (*Ap2*, *Pparγ*, *C/ebpα* and *Pgc1α*) markers was assessed by qPCR of un-induced *DKO* (orange) and *p53KO* (black) OS cells. Bars represent the mean of

NIH-PA Author Manuscript

NIH-PA Author Manuscript

NIH-PA Author Manuscript

three independent experiments (+/− SD). NS = not significantly expressed. **b**, *Rb* or control (Luc) shRNAs were expressed in the *p53KO* cell lines. *Rb* knockdown was confirmed by immunoprecipitation and qPCR showed that this caused downregulation of bone markers *Bsp* (and also *Coll1a* and *Alp*, data not shown), and upregulation of fat markers *Pparγ* (and also *Ap2* and *C/ebpα*, data not shown) without culture in differentiating media. Bars represent the mean of three independent experiments (+/− SD). **c**, The osteogenic and adipogenic potential of *shLuc*- and *shRb-p53KO* cell lines was assessed 0, 7, 14 and 21 days after differentiation induction by Alizarin Red and Oil-Red-O staining. A representative timepoint (14 days) is shown. **d**, H+E staining of representative tumors derived from *shLuc*- and *shRb-p53KO* cell lines injected subcutaneously into immunocompromised mice. *shRb-p53KO* OS cells consistently (10/10 injections) yielded tumors that arose faster, and were more aggressive, than those arising from the parental *p53KO* OS controls (10 injections). Moreover, the *shRb-p53KO* OS derived tumors were frequently (6/10 injections) mixed lineage (top inset shows fat neoplasm; bottom inset bone/undifferentiated sarcoma), while the control *shLuc-p53KO* tumors were uniformly (10/10 injections) osteosarcomas. Additional analysis of these tumors (H+E, sirius red staining and Runx2 IHC) is shown in Supplementary Figure 4.

NIH-PA Author Manuscript
NIH-PA Author Manuscript
NIH-PA Author Manuscript

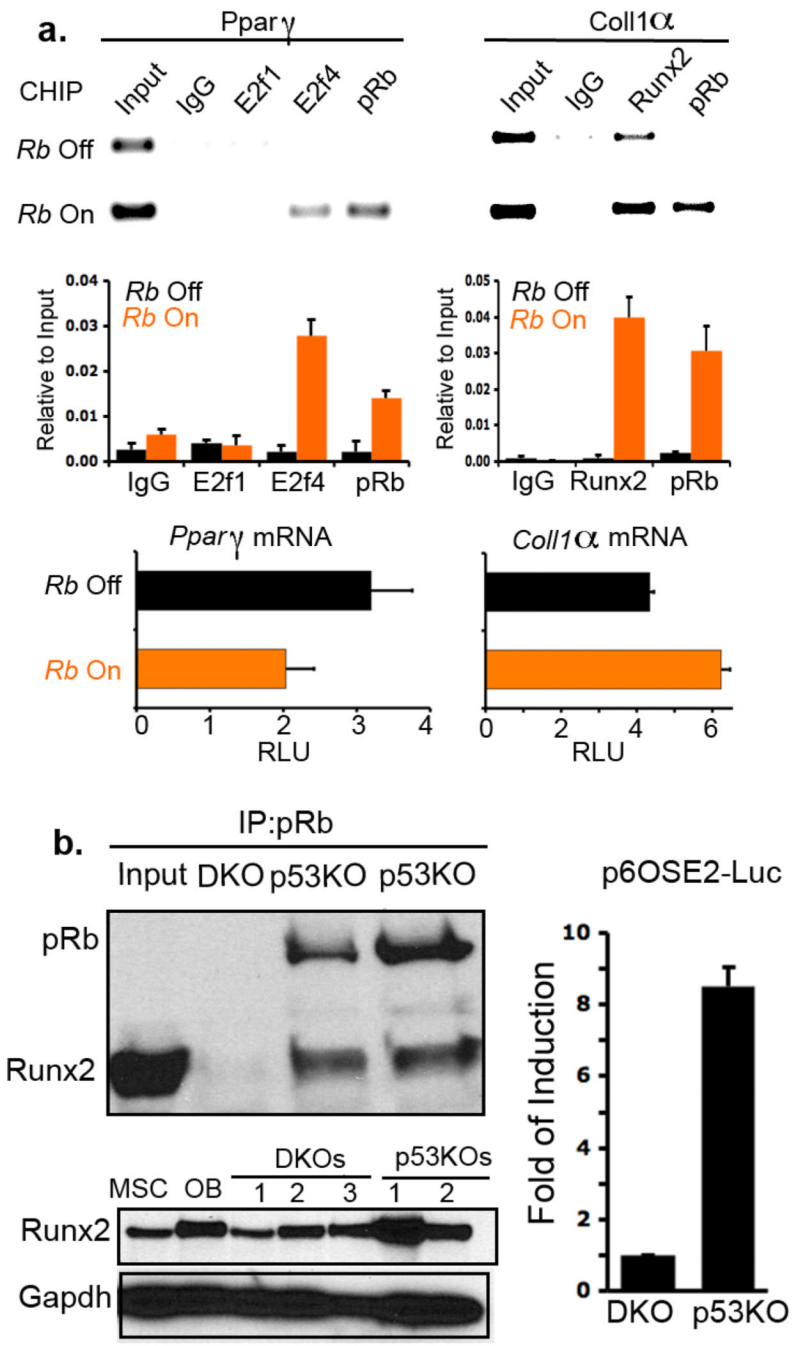

Figure 3. pRb modulates the activity and the expression of the master lineage regulators Runx2 and Pparγ

a, The stable *DKO-Rb*$^{Dox\text{-}ON}$ OS cells were generated by drug selection of pools of DKO cells transfected with the doxocyline inducible construct pCW22-Rb. These were cultured for two days in the absence (*Rb Off*) or presence (*Rb On*) of doxocycline and then analyzed. Results are representative of three independent experiments. Promoter occupancy was assessed by chromatin immunoprecipitation. Sequence analysis identified two potential E2f binding sites (−278 and −160) within the *Pparγ* promoter. pRb induction caused a dramatic upregulation of both pRb and E2F4 binding to the proximal site. (No binding was observed at the distal element.) Similarly, pRb induction allowed pRb to bind to the known Runx2

NIH-PA Author Manuscript

NIH-PA Author Manuscript

NIH-PA Author Manuscript

response element of Col1α 20 and also increased the binding of Runx2. These changes correlated with the downregulation of *Pparγ* mRNA and upregulation of Col1α mRNA as judged by qPCR. Bars represent the mean of three independent experiments (+/− SD). **b**, Western blotting detected Runx2 in pRb-immunoprecipitates from *p53KO*-OS cell lines (left, top panel). Western blotting of whole cell extracts confirmed that Runx2 was expressed in both DKO and *p53KO* OS cell lines (left, bottom panel). MSCs and osteoblasts were used as a positive control. Right panel: Runx2 transcriptional activity was shown to be higher in the *p53KO*- versus the DKO OS cell lines as judged by activation of the artificial Runx2-responsive reporter p6OSE2-Luc. Results are the average of six independent samples. Error bars indicate S.E.

NIH-PA Author Manuscript
NIH-PA Author Manuscript
NIH-PA Author Manuscript

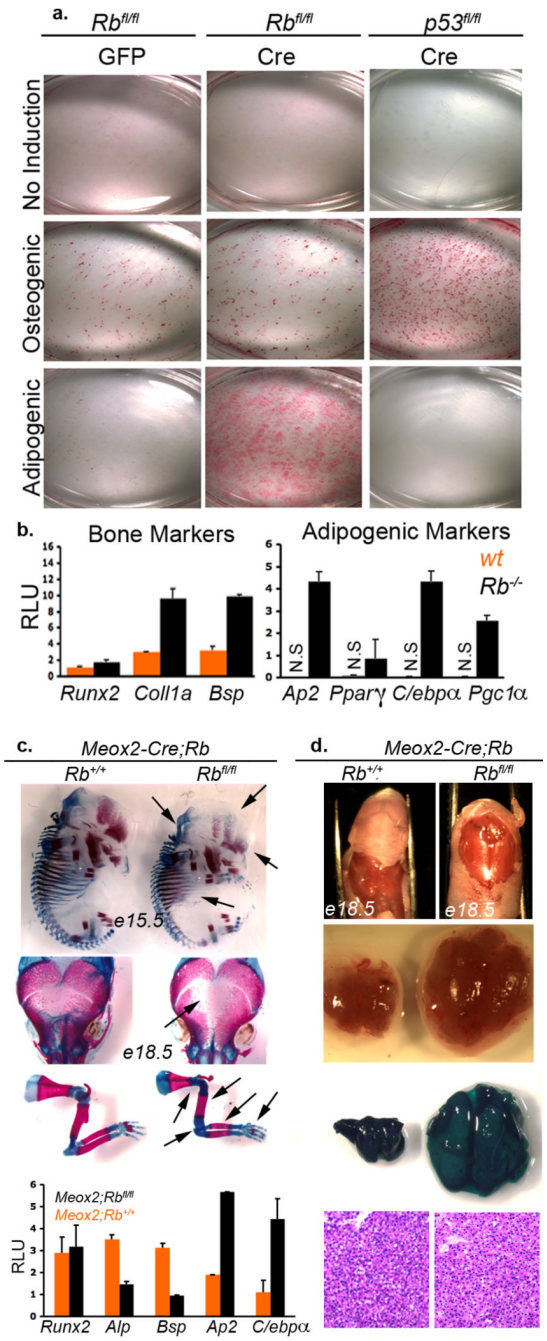

Figure 4. *Rb* maintains the osteoblastic fate commitment in normal osteoblasts and regulates fate choice during normal development *in vivo*

a, Calvarial osteoblasts were prepared from e18.5 $Rb^{fl/fl}$ or $p53^{fl/fl}$ embryos and infected with Ad-GFP or Ad-Cre at P1. Five days later, the cells were induced with differentiation media and then assayed for osteogenesis and adipogenesis at 0, 14 and 25 days by staining with Alizarin Red and Oil-Red-O. A representative timepoint (25 days) is shown. **b**, qPCR was also used to assess osteogenic and adipogenic markers in the un-induced $Rb^{fl/fl}$ (wt) versus $Rb^{fl/fl}$+Ad-Cre ($Rb^{-/-}$) osteoblasts. Bars represent the mean of three independent experiments (+/− SD). **c**, Alizarin Red (bone mineralization) and Alcian Blue (cartilage) staining of e15.5 skeletons (top panel), e18.5 calvaria (middle panel) and e18.5 limbs

NIH-PA Author Manuscript

NIH-PA Author Manuscript

NIH-PA Author Manuscript

(botton panel) from *Meox2-Cre;Rb*$^{+/+}$ and *Meox2-Cre;Rb*$^{fl/fl}$ littermate embryos. Arrows mark visible skeletal defects. qPCR was used to assess osteogenic (*Runx2*, *Alp*, and *Bsp*) and adipogenic (*Ap2* and *C/ebp*α) markers in mRNA extracted from the calvarial bones of e18.5 *Meox2-Cre;Rb*$^{+/+}$ and *Meox2-Cre;Rb*$^{fl/fl}$ embryos. Bars show the mean of three embryos arising in two independent crosses (+/− SD). **d**, Brown adipose tissue (BAT) was dissected from the backs of *Meox2-Cre;Rb*$^{fl/fl}$ embryos (n=10) and their *Meox2-Cre;Rb*$^{+/+}$ littermate controls. All 10 showed a dramatic expansion of the brown fat compartment. A representative example is shown (upper two panels). Introduction of the LSL-LacZ reporter into this model, and LacZ staining confirmed equal, widespread expression of Cre in the control and *Rb* mutant BAT (third panel). H+E staining of BAT (bottom panel).